Chemical Physics Letters 497 (2010) 30–32

Contents lists available at ScienceDirect

Chemical Physics Letters

journal homepage: www.elsevier.com/locate/cplett

Rotationally resolved $A^3\Sigma_u^- - X^3\Sigma_g^-$ spectrum of HC_7H

N. Wehres [a,b], D. Zhao [c,*], W. Ubachs [c], H. Linnartz [a,c]

[a] Sackler Laboratory for Astrophysics, Leiden Observatory, University of Leiden, P.O. Box 9513, NL 2300 RA Leiden, The Netherlands
[b] Kapteyn Astronomical Institute, University of Groningen, P.O. Box 800, NL 9700 AV Groningen, The Netherlands
[c] Institute for Lasers, Life and Biophotonics Amsterdam, De Boelelaan 1081, NL 1081 HV Amsterdam, The Netherlands

ARTICLE INFO

Article history:
Received 1 July 2010
In final form 2 August 2010
Available online 10 August 2010

ABSTRACT

The $A^3\Sigma_u^- - X^3\Sigma_g^-$ electronic spectrum of the linear carbon chain radical HC_7H has been recorded fully rotationally resolved. Cavity ring-down spectroscopy is used to record the origin band transition in direct absorption through a supersonically expanding planar plasma, discharging a diluted gas mixture of acetylene in helium. Rotational resolution is obtained by operating a commercial pulsed dye laser system in a second grating order configuration, resulting in a narrower bandwidth of about 0.035 cm^{-1}. In total, 39 resolved P- and R-branch transitions are included in a standard fit, yielding for the first time accurate rotational constants for both electronic states.

1. Introduction

Highly unsaturated carbon chain radicals have attracted much interest in recent years. Following systematic Fourier transform microwave laboratory studies [1] several carbon chains have been identified in dense interstellar clouds, varying from cyanopolyynes HC_nN as large as $HC_{11}N$ [2] to carbon chain cations (e.g., $HCCCNH^+$ [3]) and anions (e.g., C_6H^- and C_8H^- [4,5]). Matrix isolation studies [6], in addition, have guided optical gas phase surveys to record electronic transitions of pure carbon chains C_n and mixed $XC_nY^{(+/-)}$ species with X,Y = H, N, O and S containing chains, using sensitive spectroscopic detection techniques, such as REMPI-TOF, photo-detachment, cavity ring-down and plasma-frequency double modulation schemes (see [7,8] for a review). The resulting spectra have been used to compare optical spectra of carbon chains with diffuse interstellar band (DIB) positions, absorption features in the star light crossing diffuse interstellar clouds, but so far without unambiguous identifications [9,10].

One carbon chain radical that has been studied in the past is the linear triplet chain HC_7H. This is a member of the $HC_{2n+1}H$ series for which the electronic $^3\Sigma_u^- - X^3\Sigma_g^-$ bands have been recorded for $n = 2$–7 in a 5 K Ne matrix [11]. The matrix bands are broadened and their absorption frequencies are typically shifted by as much as 100 cm^{-1} compared to the gas phase – reason why these data cannot be used to compare directly with DIB positions – but as such they are indicative for where to start searching in the gas phase. Using the available matrix data, electronic spectra of HC_7H, HC_9H, $HC_{11}H$ and $HC_{13}H$ have been recorded in the gas phase [12–14]. In the case of HC_7H the matrix shift for the origin band turned out to be only 7 cm^{-1}. A clear P- and R-branch structure as typical for a Σ–Σ transition was found in Refs. [12,13], but individual transitions could not be fully resolved. As no fluorescence signals were found, a radiationless lifetime broadening of the upper state of 100 ps or longer was proposed to explain the lack of rotational resolution. A conclusive identification of the spectrum, though, was possible following a REMPI-TOF mass selective study, reporting the band head at 504.45 nm on a mass channel appropriate to HC_7H [15]. In Ref. [14] a better resolved spectrum was achieved, but only a contour fit was presented based upon a theoretically predicted ground state B-value (taking $B_0 \equiv B_e$). The present study extends the spectroscopic characterization of the $A^3\Sigma_u^- - X^3\Sigma_g^-$ origin band transition of HC_7H and provides a full rotational analysis. The use of a planar plasma source (as in Ref. [14]), providing an essentially Doppler-free environment, instead of a pinhole nozzle, and an improvement in laser bandwidth by operating a commercial pulsed dye laser system in a higher grating order, allows for recording nearly forty subsequent transitions in the $A^3\Sigma_u^- - X^3\Sigma_g^-$ origin band spectrum around 504.5 nm.

2. Experimental

The experiment is based on a pulsed cavity ring-down detection scheme, monitoring rotationally cold hydrocarbon radicals in a supersonically expanding plasma by discharging a 1% C_2H_2/He mixture. This method is well established and essentially identical to that described in detail in Refs. [8]. It is used in the present study in Amsterdam (see also Ref. [16]). More specifically the present experiment comprises a 3 cm × 100 μm slit nozzle consisting of two metal jaws that act as cathode and a slotted metal anode, separated by a slotted ceramic plate. The nozzle body is mounted to a General Valve. The nozzle is mounted in a vacuum chamber that is pumped by a roots blower system with 1000 m^3/h pumping capacity. The typical pressure in the chamber is 0.1 mbar during jet

* Corresponding author.
E-mail address: d.zhao@few.vu.nl (D. Zhao).

0009-2614/$ - see front matter © 2010 Elsevier B.V. All rights reserved.
doi:10.1016/j.cplett.2010.08.006

operation. Backing pressures are as high as 12 bar. The nozzle is mounted with its slit orifice parallel to the optical axis of a 50 cm long optical cavity, off-set by a few mm. This cavity consists of two plano-concave mirrors with an average reflection coefficient R better than 0.9999 that are mounted on high precision alignment tools. The light leaking out of the cavity is detected with a photomultiplier tube and typical ring-down times amount to 12–15 μs. A multi trigger scheme is used to synchronize the ring-down event, discharge pulse (300 μs, ~100 mA, −750 V) and gas pulse (~ 1 ms). The setup is operated at 10 Hz, which is determined by the maximum repetition rate of a tripled Nd:YAG laser that is used to pump a dye laser system (Sirah, Cobra-Stretch) with Coumarine 307 as laser dye, covering the 490–520 nm region. This commercial laser system is standard configured with a double grating resonator and has a typical best bandwidth in this wavelength range of 0.07 cm^{-1}, when operated as described in the manual. A relatively simple trick allows substantial improvement of the achievable laser resolution. For this the second order diffraction of the Littrow grating is used (instead of the first order), yielding a laser bandwidth improvement with a factor of two. I_2 reference spectra are used to determine the laser frequency and an etalon with a free spectral range of 21 GHz is used for linearization of the wavelength scan. This yields an absolute laser frequency precision better than 0.02 cm^{-1}.

3. Results and discussion

In Figure 1 (upper trace) the rotationally resolved $A^3\Sigma_u^- - X^3\Sigma_g^-$ electronic origin band spectrum of HC_7H is shown as measured here. As in the previous studies by Ball et al. [12,13], the P- and R-branch contour can be easily resolved. A Q-branch is not present. Irregularities, mainly in the P-branch, are due to overlapping transitions around 19816.2, 19816.7, 19817.0, and 19817.1 cm^{-1}, that are most likely due to C_2 Swan band transitions [17,18]. The combined application of a slit, i.e., Doppler-free expansion and a narrower band width allows the identification of individual rotational transitions, also as every second transition is hard to observe; HC_7H is a linear centro-symmetric molecule with nuclear statistical weights 1:3 for symmetric and asymmetric rotational levels, respectively, and as a consequence, mainly transitions starting from asymmetric levels are observable, resulting in an effective line splitting of the order of 4B, instead of 2B. In addition, each rotational level in both the ground and excited $^3\Sigma$ state is split into three fine structure levels that are defined by the total angular momentum J with $J = N + 1$, N and $N - 1$ (except for $N = 0$ where $J = 1$). This spin structure is not resolved but determines, to some extent, the spectral appearance of individual transitions, particularly in the band origin region, as the spin–spin fine structure is most prominent in the lowest rotational states. In total 39 transitions, equally divided over P-branch (19) and R-branch (20) are resolved and the transition frequencies are listed in Table 1. In both the figure and the table the rotational assignment is indicated. All transitions were fitted using PGopher [19] and a standard Hamiltonian for a $^3\Sigma - ^3\Sigma$ transition, with the band origin ν_{00}, rotational and centrifugal distortion constants, B_0'', D_0'' and B_0' and D_0', in ground and excited state as parameters. Inclusion of distortion effects is essential to decrease the overall error of the fit that amounts to ~0.01 cm^{-1}, i.e., well below the improved bandwidth of the laser. The resulting constants are listed in Table 2 and the resulting observed–calculated values are given in Table 1.

In Figure 1, the simulated spectrum is shown for these constants for a line width of 0.04 cm^{-1} (lower trace). The observed spectrum resembles that of the iso-electronic cyanopolyyne HC_6N [14] and dicyanopolyyne, C_5N_2 [20]. Both these molecules have been studied previously in a similar way, also combining cavity ring-down spectroscopy and supersonic planar plasma expansions. The origin band transitions of these bands are close to that for HC_7H, as one may expect for chains of comparable length. Also the other constants are of the same order and are listed for comparison in Table 2.

A good estimate for the ground state rotational constant is possible from theoretical calculations [21], yielding $B_e'' = 0.0279$ cm^{-1}. We performed a new calculation at the B3lyp/6-311++G** level using the Gaussian 98 software [22], yielding an improved value of $B_e'' = 0.02816$ cm^{-1}. This value is close to the ground state value $B_0'' = 0.0283263$ cm^{-1}, as derived here. The B_0''/B_0' ratio amounts to

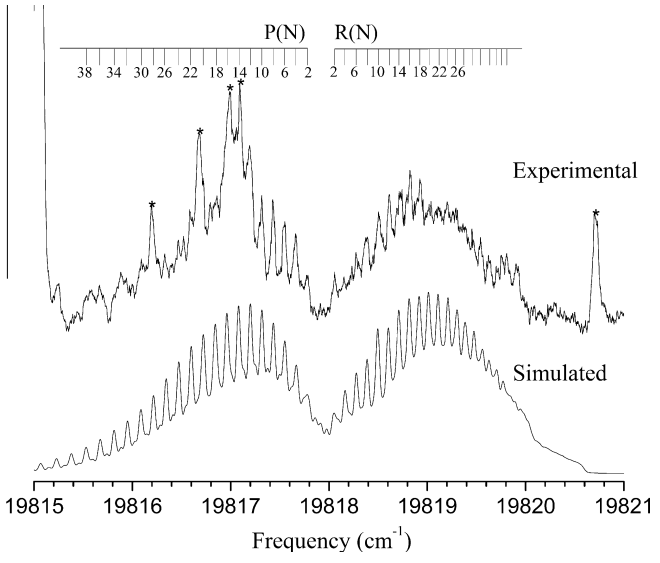

Figure 1. The rotationally resolved $A^3\Sigma_u^- - X^3\Sigma_g^-$ electronic transition of HC_7H recorded by cavity ring-down spectroscopy through expanding planar plasma by discharging a high pressure mixture of 1% C_2H_2 in He (upper trace). Simulated spectra are shown in the lower trace for a linewidth of 0.04 cm^{-1} and a rotational temperature of 18 K. Irregularities, marked by an asterisk, are likely due to overlapping C_2 transitions.

Table 1
Observed rotationally resolved transitions of the $A^3\Sigma_u^- - X^3\Sigma_g^-$ electronic origin band transition of HC_7H.

N″	P-branch transitions		R-branch transitions	
	Observed (cm^{-1})	$o-c$[a] (10^{-3} cm^{-1})	Observed[a] (cm^{-1})	$o-c$[a] (10^{-3} cm^{-1})
2	19817.778	−1	19818.058	−3
4	19817.661	−3	19818.160	−12
6	19817.547	−2	19818.276	−7
8	19817.433	−1	19818.390	−2
10	19817.316	−2	19818.505	5
12	19817.203	3	19818.614	8
14	19817.09[b]	7	19818.712	−1
16	19816.97[b]	7	19818.818	3
18	19816.854	12	19818.925	9
20	19816.720	−1	19819.024	8
22	19816.593	−4	19819.121	9
24	19816.469	−4	19819.204	−2
26	19816.33[b]	−15	19819.289	−8
28	19816.22[b]	−3	19819.373	−12
30	19816.092	5	19819.457	−10
32	19815.94[b]	−9	19819.539	−7
34	19815.82[b]	−1	19819.636	4
36	19815.67[b]	−8	19819.701	11
38	19815.53[b]	−2	19819.755	−3
40			19819.809	−2

[a] The observed-calculated ($o-c$) are derived using the constants listed in Table 2.
[b] Blended transitions. A weight factor including a roughly three times lower accuracy of the frequency determination was used in the fitting routine.

Table 2
Derived constants of the $A^3\Sigma_u^- - X^3\Sigma_g^-$ electronic transition of HC_7H and a comparison with the iso-electronic species HC_6N and NC_5N. All values are in (cm^{-1}).

	HC_7H	HC_6N [14]	NC_5N [20]
$\nu_{00\ matrix}$	19 824 [11]	21 181	22737.3
$\nu_{00\ gas}$	19817.892(2)	21208.60(5)	22832.7(1)
Matrix shift	6	28	95
B_0''	0.0283263(48)	0.02806299(2)	0.02799(4)
D_0'' (10^{-7})	2.217(39)	–	–
B_0'	0.0282298(46)	0.02792(5)	0.02778(3)
D_0' (10^{-7})	2.812(36)	–	–
B_0''/B_0'	1.0034	1.0051	1.0076

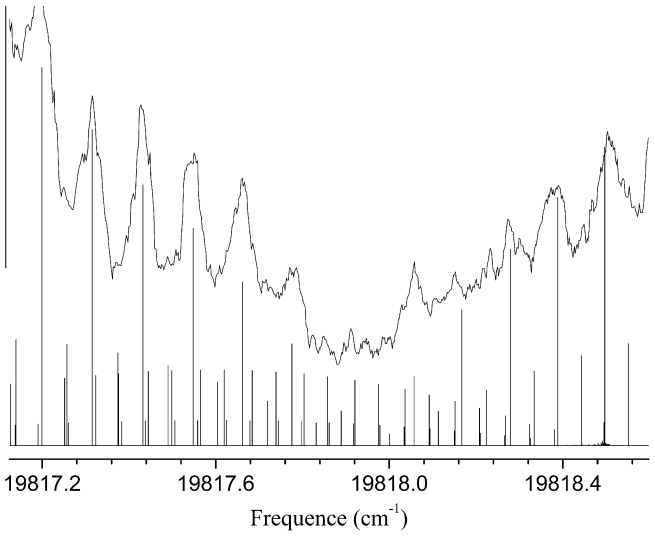

Figure 2. The band origin region of the $A^3\Sigma_u^- - X^3\Sigma_g^-$ electronic origin band spectrum of HC_7H (upper trace) with simulated stick diagram (lower trace). The stick diagram, in the band gap region strongly depending on the choice of the λ-constants, demonstrates the spectral fading when rotational lines and spin–spin splittings do not coincide.

1.0034 and reflects a small lengthening of the chain upon electronic excitation. This value is slightly lower than the values found for HC_6N (1.0051) and NC_5N (1.0076). The (fitted) band origin is located at 19817.892(1) cm^{-1}, which is about 0.1 cm^{-1} (0.03 cm^{-1}) red shifted from the value reported in Ref. [13] ([14]). This is well within the reported uncertainties with which the absolute frequencies could be determined.

A precise fit of the overall band contour, particularly of the band gap area, also requires knowledge of the spin–spin coupling constants in both ground and excited state. As shown in Figure 2, each resolved peak consists of at least three close lying components with a quantum labeling that strongly depends on the spin–spin interaction. As the final resolution does not allow resolving irregularities because of interference of triplet splittings, this is hard to realize. From the fit a difference between the spin–spin constants for the ground and excited state – $\Delta\lambda = \lambda' - \lambda''$ - of about 0.27 cm^{-1} can be estimated. The actual values are more difficult to determine. In previous Letters (see [23]), the ground state spin–spin constant was adapted to that of the iso-electronic HC_6N (as available from FTMW work): $\lambda'' = 0.36\ cm^{-1}$. However, with this value it is not possible to reproduce the present HC_7H band profile; an empirical contour fit actually yields λ''-values that are closer to 10 cm^{-1} than to 1 cm^{-1}. Within this constraint, assuming a final rotational temperature of 18 K and a Gaussian linewidth of 0.04 cm^{-1}, the band contour can be well reproduced (see Fig. 1). The latter value is interesting, as it puts an additional limit on the lifetime of the excited state. In Ref. [13] additional line broadening (0.04 cm^{-1}) was found in excess of that (0.066 cm^{-1}) expected from the laser linewidth and Doppler width in a pin hole expansion. A rapid radiationless transition from the upper state was taken to derive a lower boundary for the lifetime τ of the order of 0.1 ns. The absence of fluorescence signals yielded an upper limit, resulting in 0.1 ns < τ < 1 ns. The present study with FWHMs of the order of 0.035 cm^{-1} narrows down this range: 0.6 ns < τ < 1 ns.

Finally, the band studied here has been compared with the newest (and substantially extended) list with DIBs [24]. The region around the $A^3\Sigma_u^- - X^3\Sigma_g^-$ electronic origin band spectrum (504.5 nm) is remarkably empty in the astronomical spectrum and HC_7H does not appear to be a good candidate for a carrier of a DIB, even not in the extended list.

Acknowledgement

We acknowledge financial support through NOVA, the Netherlands Research School for Astronomy, and the FP6 Research Training Network 'the Molecular Universe', as well as stimulating discussions with Prof. A.G.G.M. Tielens.

References

[1] M.C. McCarthy, P. Thaddeus, Chem. Soc. Rev. 30 (2001) 177.
[2] M.B. Bell, P.A. Feldman, M.J. Travers, M.C. McCarthy, C.A. Gottlieb, P. Thaddeus, Astrophys. J. 483 (1997) L61.
[3] C.A. Gottlieb, A.J. Apponi, M.C. McCarthy, P. Thaddeus, H. Linnartz, J. Chem. Phys. 113 (2000) 1910.
[4] M.C. McCarthy, C.A. Gottlieb, H. Gupta, P. Thaddeus, Astrophys. J. 652 (2006) L141.
[5] S. Brunken, H. Gupta, C.A. Gottlieb, M.C. McCarthy, P. Thaddeus, Astrophys. J. 664 (2007) L43.
[6] J.P. Maier, J. Phys. Chem. A 102 (1998) 3462.
[7] E.B. Jochnowitz, J.P. Maier, Ann. Rev. Phys. Chem. 59 (2008) 519.
[8] H. Linnartz, in: G. Berden, R. Engeln (Eds.), Cavity Ring-down Spectroscopy – Techniques and Applications, Blackwell Publishers, 2009, pp. 145–179.
[9] T. Motylewski et al., Astrophys. J. 531 (2000) 312.
[10] H. Linnartz et al., Astron. Astrophys. 511 (2010) L3.
[11] J. Fulara, P. Freivogel, D. Forney, J.P. Maier, J. Chem. Phys. 103 (1995) 8805.
[12] C.D. Ball, M.C. McCarthy, P. Thaddeus, Astrophys. J. 523 (1999) L89.
[13] C.D. Ball, M.C. McCarthy, P. Thaddeus, J. Chem. Phys. 112 (2000) 10149.
[14] O. Vaizert, T. Motylewski, M. Wyss, E. Riaplov, H. Linnartz, J.P. Maier, J. Chem. Phys. 114 (2001) 7918.
[15] H. Ding, T.W. Schmidt, T. Pino, A.E. Boguslavskiy, F. Guthe, J.P. Maier, J. Chem. Phys. 119 (2003) 814.
[16] E. Witkowicz, H. Linnartz, C.A. de Lange, W. Ubachs, A. Sfounis, M. Massaouti, M. Velegrakis, Int. J. Mass Spectrom. 232 (2004) 25.
[17] G.M. Lloyd, P. Ewart, J. Chem. Phys. 110 (1999) 385.
[18] C.V.V. Prasad, P.F. Bernath, Astrophys. J. 426 (1994) 812.
[19] PGOPHER, A Program for Simulating Rotational Structure, C.M. Western, University of Bristol, Available from: http://pgopher.chm.bris.ac.uk.
[20] H. Linnartz, O. Vaizert, P. Cias, L. Grueter, J.P. Maier, Chem. Phys. Lett. 345 (2001) 89.
[21] K. Aoki, S. Ikuta, J. Mol. Struct.: Theochem. 310 (1994) 229.
[22] M.J. Frisch, G.W. Trucks, H.B. Schegel, et al., GAUSSIAN 98, Gaussian Inc., Pittsburgh, PA, 1998.
[23] V.D. Gordon, M.C. McCarthy, A.J. Apponi, P. Thaddeus, Astrophys. J. 540 (2000) 286.
[24] L.M. Hobbs et al., Astrophys. J. 705 (2009) 32.